

# Structural improvement of strengthened deck panels with externally bonded plates

Jongsung Sim, Hongseob Oh\*

*Department of Civil and Environmental Engineering, Hanyang University, 1271 Sa1-dong, Ansan 425-791, South Korea*

Received 23 June 2003; accepted 11 August 2004

## Abstract

Concrete bridge decks require eventual replacement and rehabilitation due to decreasing load-carrying capacity. This paper compares different strengthening design procedures that improve the usability and structural performance of bridge decks. The failure characteristics of bridge decks strengthened with various materials such as carbon fiber sheet, glass fiber sheet, steel plate, and grid CFRP and GFRP are analyzed, and the theoretical load-carrying capacities are evaluated using traditional beam and yield line theory, and punching shear analysis. The strengthening materials increase the punching shear strength of the deck and change the failure mode of the strengthened panel.  
© 2004 Elsevier Ltd. All rights reserved.

*Keywords:* Fiber reinforced polymer plastic; Concrete bridge deck; Yield line theory, punching shear analysis; Structural strengthening

## 1. Introduction

External strengthening has been applied to many deteriorated bridge decks after almost 20 years of service in Korea. These decks were originally designed to support traffic loads of less than 30 tons, but traffic loads have increased to 40 tons. Therefore, old 18-cm-thick bridge decks, originally designed for relatively low traffic loads, must be strengthened with a view to restoring the entire decreased structural capacity, including load-carrying capacity and serviceability, to improve their specified structural performance.

Decks that have been externally strengthened with fiber-reinforced polymers (FRPs) or steel plates may exhibit punching shear failure, depending on the amount of strengthening or on the applied strengthening material, while conventional concrete deck panels exhibit flexural failure [1,2]. In the case of over-strengthened deck panels, the reinforcing steel bars do not yield when punching shear

failure occurs. The strengthening design of bridge decks, based on classical Westergaard theory [3], does not provide a sufficient estimate of their structural behavior when they fail, which may be due either to biaxial bending or to punching shear. Therefore, punching shear analysis and yield line theory must be used to analyze strengthened decks [4–6].

Nowadays, many different types of materials are used to strengthen deteriorated decks, such as steel plate or FRP plastic. Steel plate was most commonly used in the past as a flexural strengthening material [7,8], but its use in concrete structures has gradually declined because of its workability in situ and mechanical characteristics, including corrosion and heavy weight, despite the fact that its material properties are similar to reinforcing steel bar. For the last 20 years, research has concentrated on developing new strengthening materials that can be used as an alternative to steel plate. Carbon fiber reinforced polymer (CFRP) and glass fiber reinforced polymer (GFRP) sheets that are woven in only one direction by the manufacturer and then impregnated in place have been developed and are now widely used in Korea. The most important factor affecting the strengthening efficiency of external strengthening technique with FRP sheets, which includes characteristics such as structural

\* Corresponding author. Tel.: +82 11 9087 3085; fax: +82 31 400 4567.

*E-mail address:* [opera69@chollian.net](mailto:opera69@chollian.net) (H. Oh).

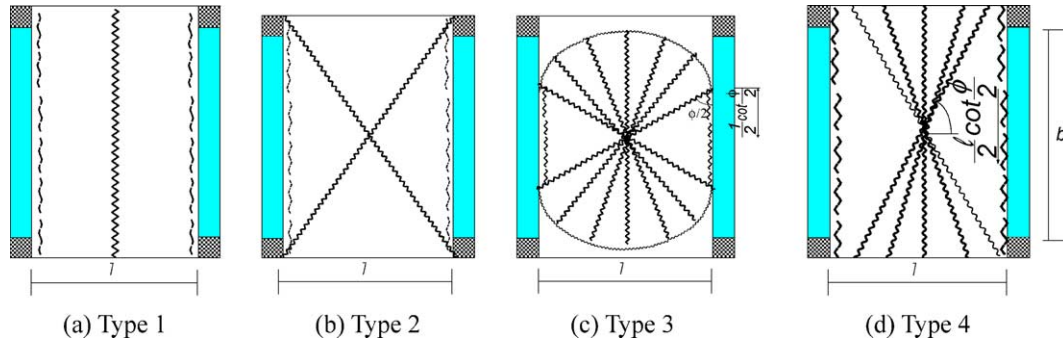


Fig. 1. Assumed yield line patterns of deck.

performance and durability, is the construction accuracy of these FRP sheets, which depends mainly on the workmanship. The consistency of the fiber direction on the concrete surface after strengthening, and the existence of voids between the concrete and fiber sheets caused by poor bonding, may affect the construction accuracy of FRPs. Recently, FRP rod and FRP grid have been exploited and used for strengthening because they are convenient and exhibit improved mechanical properties over steel plate and existing fiber sheets [9]. However, overlaid mortar and additional anchor bolts are required to bond these materials to a concrete surface. The bolts are also required to effectively distribute the tensile stress to the FRPs when flexural cracking occurs in the mortar overlay and concrete.

This paper compares the structural performance of bridge decks strengthened with various materials, such as steel plates, CFRP sheets, GFRP sheets, and rod and grid CFRP sheets. It also analyzes the theoretical strength of the decks based on beam and yield line theory, and punching shear analysis.

## 2. Strengthening design

The flexural design of deck panels was analyzed using traditional beam and yield line theory, as well as punching shear analysis, to estimate their theoretical load-carrying capacity.

In traditional beam theory, when a strengthening material is applied to the tension face, the combined nominal flexural capacity becomes

$$M_n = A_s f_y \left( d - \frac{A_s f_y + A_{PLATE} f_{PLATE}}{1.7 f_c' b} \right) + A_{PLATE} f_{PLATE} \left( h - \frac{A_s f_y + A_{PLATE} f_{PLATE}}{1.7 f_c' b} \right) \quad (1)$$

where  $A_{PLATE}$  is the cross-sectional area of the strengthening material per unit width,  $b$  is a width of beam,  $h$  is the total slab thickness,  $f_c'$  and  $f_y$  are the compressive strength of concrete and the yield strength of steel rebar, respectively, and  $f_{PLATE}$  is the ultimate strength of strengthening material. The average stress at failure is assumed to be

equal to 80% of the ultimate strength of the material,  $f_{PLATE}$  [10].

According to the Korean Highway Design Specifications [10], the transverse moment due to a concentrated wheel load  $P$  is given by

$$M = \frac{(L + 0.6)P(1 + IM)}{9.6} \quad (2)$$

where  $L$  is the clear span length between girders (in meters) and  $IM$  is the impact factor. Eq. (2) is based on classical elastic beam theory [3].

According to yield line theory, yield line patterns can be classified into four types as depicted in Fig. 1: type 1 involves the panel failing as a wide beam, type 2 is composed of triangular shaped segments, type 3 is composed of two circular pans, and type 4 is a combination of types 2 and 3 [11].

The solutions based on the yield line theory may need to be modified if there is an in-plane shear crack or a diagonal crack in the deck due to flexure. Any substantial relative motion of the two crack faces may introduce kinking of the FRP bands, which reduces the contribution of the FRP to the ultimate flexural strength of the section, because of the reorientation of the fibers. The reduction factor will be  $\cos \alpha$ , where  $\alpha$  is the angle between the normal to the crack and the fiber direction. The yield moment of the strengthened deck is defined as the strength at which the tensile reinforcing steel bars in the deck yield. Then, the yield moment and ultimate moment capacity per unit width can be computed as follows:

$$M_{xy} = A_s f_y \left( d - \frac{A_s f_y + A_{PLATE} f_{PLATE}}{1.7 f_c' b} \right) + A_{PLATE} f_{PLATE} \left( h - \frac{A_s f_y + A_{PLATE} f_{PLATE}}{1.7 f_c' b} \right) \quad (3)$$

$$M_{ux} = A_s f_y \left( d - \frac{A_s f_y + A_{PLATE} 0.8 f_{PLATE} \cos \alpha}{1.7 f_c' b} \right) + A_{PLATE} 0.8 f_{PLATE} \cos \alpha \times \left( h - \frac{A_s f_y + A_{CFS} 0.8 f_{PLATE} \cos \alpha}{1.7 f_c' b} \right) \quad (4)$$

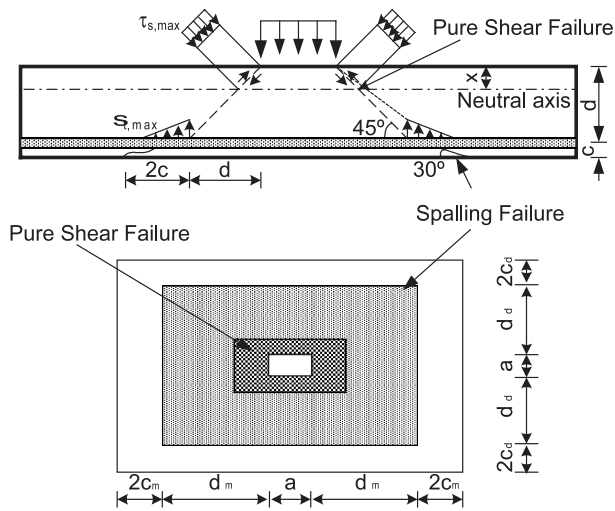


Fig. 2. Matsui's punching shear model [12].

where  $f_{\text{PLATE}}$  is the stress of the strengthening material when the rebar starts to yield.

The theoretical punching shear analysis suggested by Matsui [12], as shown as Fig. 2, was also performed to predict punching shear failure, which constitutes one of the dominant failure patterns of bridge decks. This analysis is required, because previous research has found that the shear strength given by the ACI specification is less than the actual shear strength. Matsui evaluated the static and fatigue behavior of concrete decks experimentally and proposed a punching shear model as follows [12]:

$$P_o = \tau_{s\max}[2(a + 2x_m)x_d + 2(b + 2x_d)x_m] + f_{i\max}[2(4C_d + 2d_d + b)c_m + 2(a + 2d_m)C_d] \quad (5)$$

$$\tau_{s\max} = 0.252f'_c - 0.000246f'_c{}^{1/2} \text{ [kgf/cm}^2\text{]} \quad (6)$$

$$f_{i\max} = 0.583f'_c{}^{1/2} \text{ [kgf/cm}^2\text{]} \quad (7)$$

where  $a$  and  $b$  are the width and length of the tire contact area,  $x_m$  and  $x_d$  are the distance to the neutral axis in the transverse and longitudinal directions,  $d_m$  and  $d_d$  are the distance from the transverse and longitudinal tension steel to the compression face,  $C_m$  and  $C_d$  are the concrete cover in the transverse and longitudinal directions,  $\tau_{s\max}$  is the direct shear strength of the concrete based on the test results, and  $f_{i\max}$  is the tensile strength of the concrete.

### 3. Test program

#### 3.1. Test setup

For the experimental test program, a prototype deck panel with dimensions of 160×240 cm was selected to simulate a real bridge deck supported by two girders, as shown in Fig. 3. The slab thickness was 18 cm, which is the

same as that of bridge decks in Korea. The 28-day compressive strength of the concrete was 22.5 MPa, which is similar to that of actual deteriorated bridge decks constructed in 1970s. The tensile rebar spacing in the transverse direction was 10 cm and the reinforcement spacing in the longitudinal direction was 15 cm. The preliminary designs for the reference deck panel and strengthened deck panel were developed using the Korean Highway Design Specifications, based on traditional beam theory. The material properties are listed in Table 1. In this study, steel plate, carbon fiber sheet, CFRP rod, CFRP grid, GFRP plate and glass fiber sheet were used for strengthening materials, GFRP plate is laminated with eight layers in two directions, CFRP and GFRP sheets, respectively, only woven in one direction. In Table 1, 'I' indicates that the specimen was strengthened isotropically, and 'TA' indicates that the specimen was strengthened only in the transverse direction. The strengthening scheme is illustrated in Fig. 4 (see also Table 2); that is, the CF sheets and GF sheets are applied only in strips have 10-cm width. When strengthening the section, it is useful to introduce a so-called strengthening ratio, defined as  $A_{\text{CFRS}}/hb$  as represented in Table 2. Strengthening amounts of each material is considered the specification suggested by manufacturer and also based on the elastic beam theory.

Figs. 3 and 4 also show the positions of the strain gages and LVDTs that were used to measure the strains of the reinforcing bar and strengthening materials, and the deflections. The static load was applied by a 2000-kN capacity hydraulic jack to an area of 25×50 cm at the deck

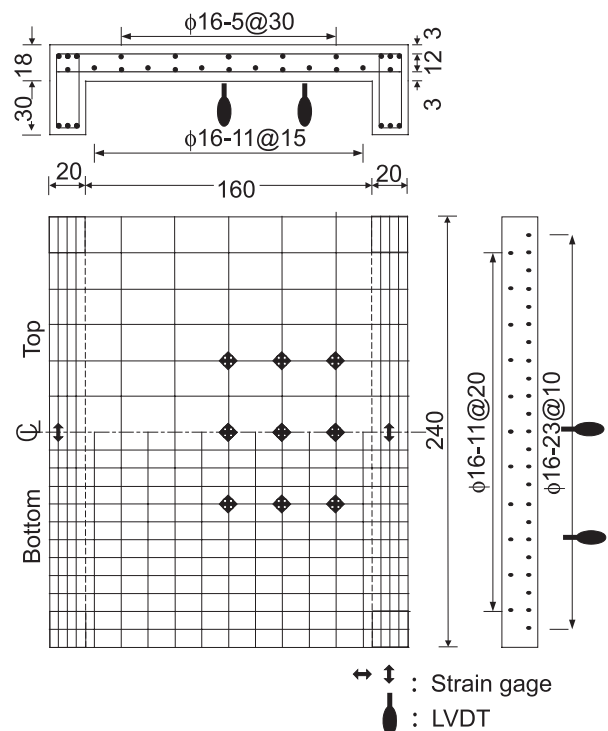


Fig. 3. Details of specimen (unit: cm).

Table 1  
Material properties

	Abbreviation	Thickness or diameter	Yield strength (MPa)	Ultimate strength (MPa)	Elastic modulus (MPa)	Ultimate strain
Concrete			–	22.5	$0.232 \times 10^5$	–
Rebar		$\phi=13$ mm	300	400	$1.96 \times 10^5$	–
Epoxy			–	88.3	$0.07 \times 10^5$	–
Steel plate	SP	$t=4.5$ mm	240	280	$1.96 \times 10^5$	–
Glass fiber reinforced polymer plastic	GP	$t=8.0$ mm	–	300	$0.25 \times 10^5$	0.012
Carbon fiber sheets	CF	$t=0.11$ mm	–	3,500	$2.31 \times 10^5$	0.015
Glass fiber sheets	GF	$t=1.3$ mm	–	450	$0.227 \times 10^5$	0.02
Carbon fiber rod	CFR	$\phi=6$ mm	–	2,352	$1.20 \times 10^5$	0.0115
Mortar for CFR			–	45.0	$0.108 \times 10^5$	–
GCFRP	GCFRP	$t=4.0$ mm	–	1,170	$1.00 \times 10^5$	0.0117
Mortar for GCFRP			–	27.0	$0.14 \times 10^5$	–

center to simulate the tire contact area of an actual vehicle. During the test, the displacements and strains in the strengthening material and reinforcing bars were measured and automatically recorded by the data acquisition system.

All 10 deck panels were loaded, unloaded, and reloaded at every 100 kN, up to 700 kN.

The differences in strengthening procedures between steel plate and FRP materials are depicted in Fig. 5. The

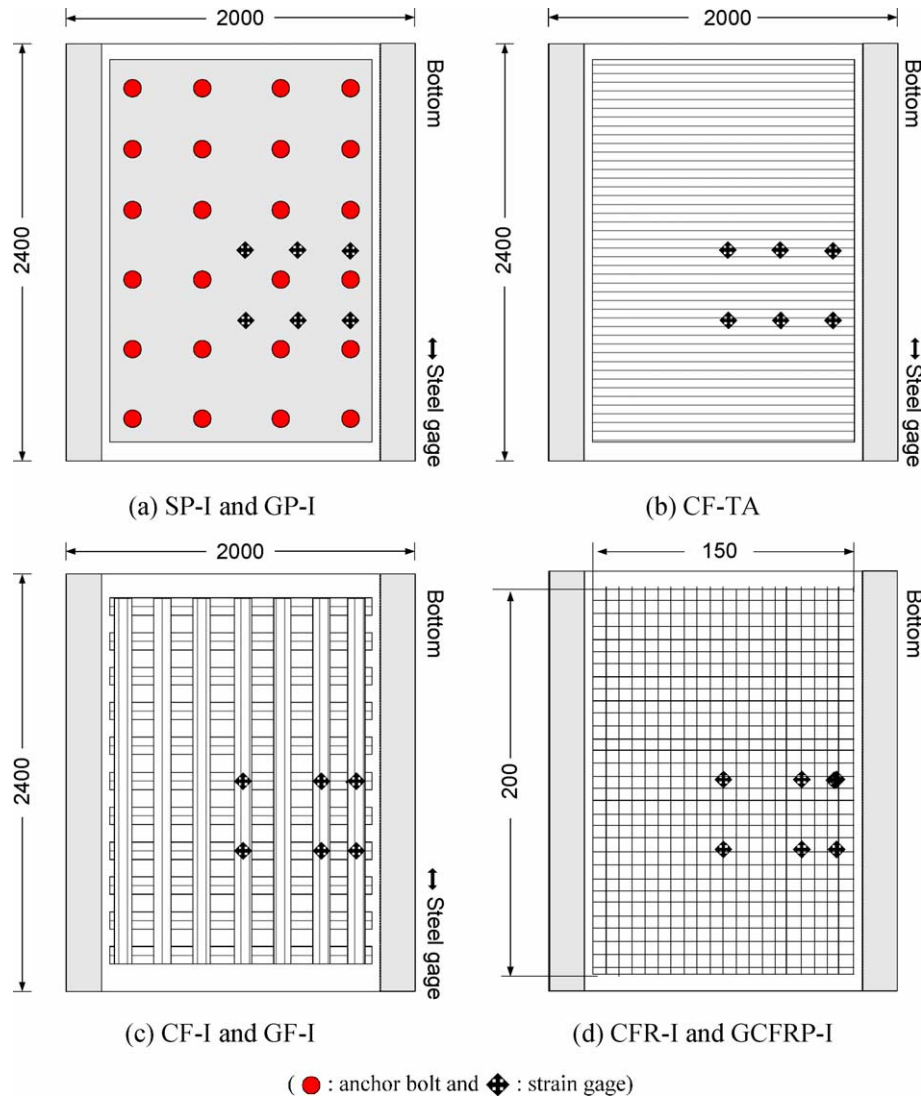


Fig. 4. Strengthening details and gage position.

Table 2  
Experimental variables

Specimen	Preload (kN)	Strengthening ratio ( $\frac{A_{PLATE}}{hb}$ ) and scheme		Note
		Transverse	Longitudinal	
CON	–	–	–	Reference
SP-I	150	2.5%, soffit area		Anchor bolts and epoxy injecting
SP-I-H	270			
GP-I	150	4.4 %soffit area		Anchor bolts and epoxy injecting
CF-TA	150	0.12%, soffit area	–	Epoxy coating
CF-I	150	0.061%, 10 cm sheet width×2 plies×5 strips per unit width	0.061%, 10 cm sheet width×2 plies×5 strips per unit width	Epoxy coating
GF-I-N	–	0.65%, 10 cm sheet width×2 plies×5 strips per unit width	0.65%, 10 cm sheet width×2 plies×5 strips per unit width	Epoxy coating
GF-I-H	270			
CFR-I	150	0.34%, $\phi 6$ at 4 cm per unit width	0.34%, $\phi 6$ at 4 cm per unit width	Anchor clip to hold bars and mortar overlay
GCFRP-I	150	0.18%, 17.6 cm <sup>2</sup> at 5 cm per unit width	0.18%, 17.6 cm <sup>2</sup> at 5 cm per unit width	Anchor bolts to hold GCFRP and mortar overlay

applied strengthening procedures and used materials shown in Fig. 5 and Table 2 are followed in the specifications suggested by each manufacturer. Deck panels SP-I and GP-I were bonded by injecting epoxy into the interface between the plate and concrete surface, after the plate had been anchored with bolts to prevent delamination. The thickness of the adhesive used for the steel plate and GP was 3 and 8 mm, respectively. The anchor bolts used for the SP material were inserted to a depth of 3 cm (equal to the concrete

cover) every 40 cm in both directions. The depth of the anchor bolts for the GP-I panels was 8 cm; the spacing was the same as that used for the SP material. Each strengthening material was applied according to the manufacturer’s specifications. An SP thickness of 4.5 mm was adopted because epoxy injection may cause the plate to deform as suggested by the manufacturer.

The CF sheets and GF sheets were bonded to the prototype deck panel in an upside-down position. Each



(a) Installation of anchor bolts



(a) Bonding of FRP sheets



(a) Installation of anchor clips or anchor bolts



(b) Injection of epoxy



(b) Over-coating by resin



(b) Application of polymer mortar overlay

Plate Type

(Steel plate and Glass fiber Reinforced polymer plate)

Sheet Type

(Carbon fiber sheet and Glass fiber sheet)

Plastic Type

(Carbon fiber rod and carbon fiber reinforced polymer grid)

Fig. 5. Strengthening procedures.

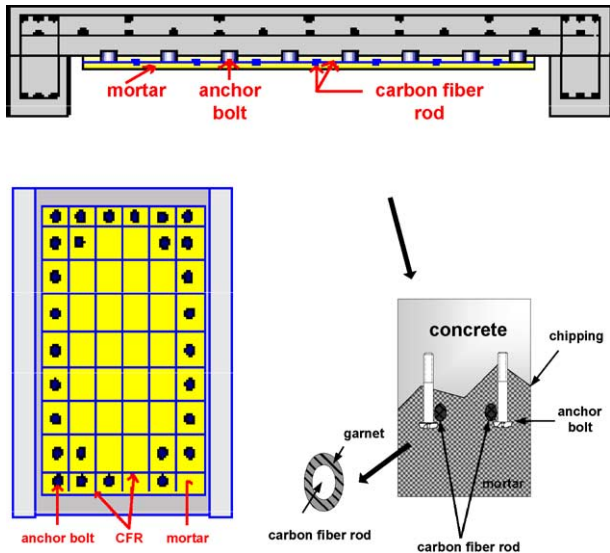


Fig. 6. Strengthening scheme carbon fiber rods and position of anchor bolts.

fiber sheets was attached to the epoxy-coated surface by pressing it into the epoxy. The thickness of CF and GF in Table 1 means only the thickness of fiber sheets. The FRP of test panels CFR-I and GCFRP-I was first embedded on the concrete surface in an upside-down position. An anchor clip that was fixed to only one end of the CFR was used for panel CFR-I, whereas 2.5-cm deep anchor bolts, depicted in Fig. 6, were used for panel GCFRP-I. Then, the reinforcing material was overlaid using a mortar suggested by the manufacturer. The mortar overlay used for the strengthening with CFR is different from the mortar for GCFRP.

Each test panel was pre-loaded to simulate structural deterioration by tension cracks prior to strengthening. In particular, panels SP-I-H and GF-I-H were pre-loaded to 270 kN, which is almost 60% of the transverse rebar yielding load in an unstrengthened test panel, based on the test result of panel CON.

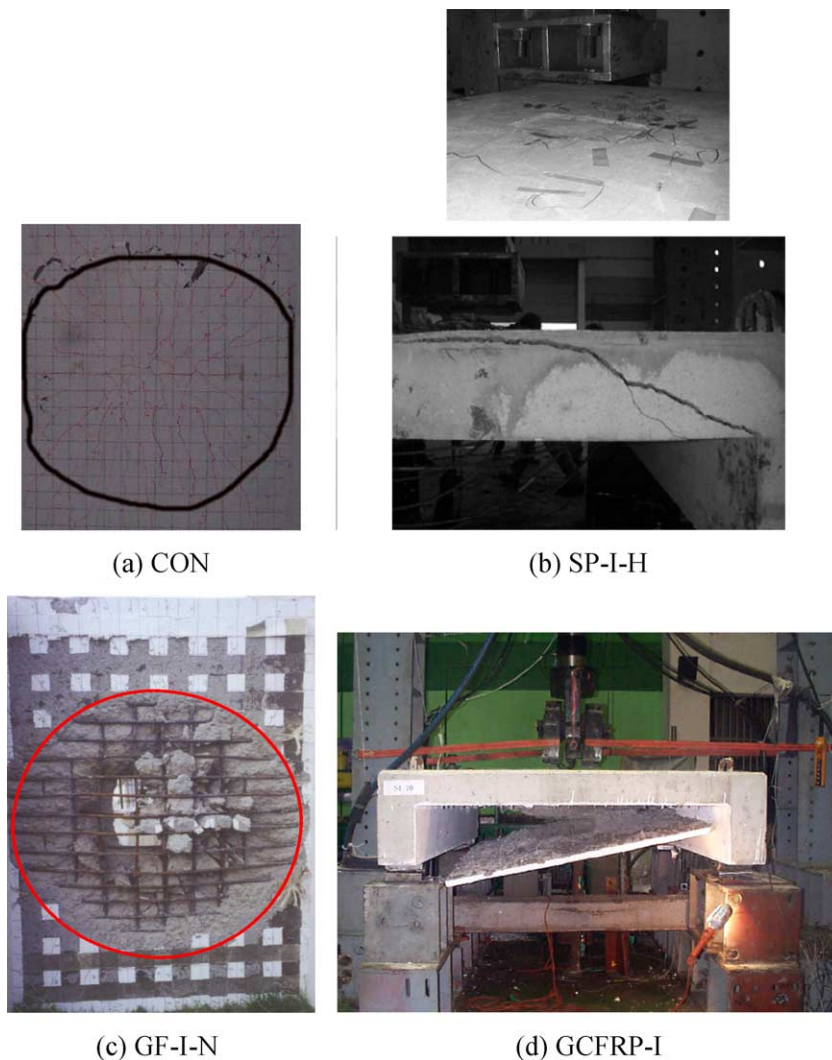


Fig. 7. Typical failure patterns.

3.2. Failure patterns

Fig. 7 illustrates the typical failure patterns of the test panels. Panel CON depicted in Fig. 7(a) exhibited punching shear failure after the reinforcing bars yielded in both direction in the mid-span. Initial cracks developed in the longitudinal direction at a load of 150 kN. As the load increased further, transverse cracks also appeared, propagating from the additional longitudinal cracks up to failure. At the punching cone of the panel, the angle of the punching shear crack above the rebar was 35°.

The crack patterns in concrete panels SP-I, SP-I-H, and GP-I were examined after the strengthening material had been removed. Panels SP-I and SP-I-H also exhibited brittle punching shear failure, as shown in Fig. 7(b). The difference in the load-carrying capacity of panels SP-I and SP-I-H was insignificant: SP-I was 10% higher than SP-I-H. The failure of panel GP-I was very similar to that of panel SP-I.

Panel CF-TA developed a noticeable initial crack at 300 kN that was parallel to the transverse CFS. As the load increased further, cracks propagated from the initial crack in only the transverse direction, parallel with the carbon fiber sheets, until punching shear failure occurred. These cracks were caused by overstrengthening in the transverse direction. The cracking patterns of panels CF-I, GF-I-N, and GF-I-H were very similar. As in the reference panel CON, cracks propagated towards the deck edges. After the steel reinforcement yielded in both directions, partial interface debonding of the carbon fiber sheets was observed. All of the panels that were strengthened with FRP sheets ultimately failed due to punching shear after the rebar in mid-span yielded in both direction, as shown in Fig. 7(c).

The crack patterns of panels CFR-I and GCFRP-I were similar to those of the reference panel, but the crack width and spacing in the mid-span of the deck were much less. The tensile stresses of the deck were well distributed in both directions by the closely embedded FRPs, and were controlled so that they did not exceed the tensile strength of the concrete. These results indicate that the cracks in a strengthened slab depend on the spacing of the strengthen-

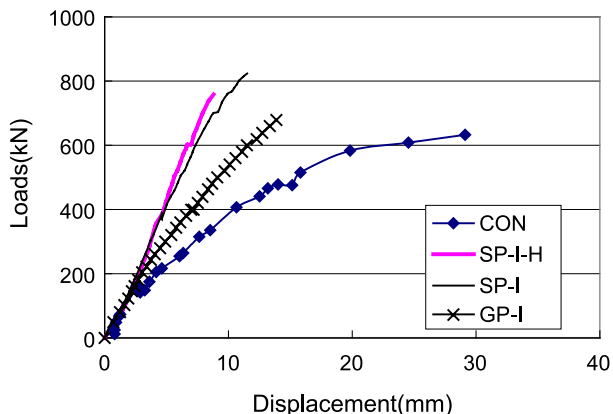


Fig. 8. Load–displacement relationship of decks strengthened with plates.

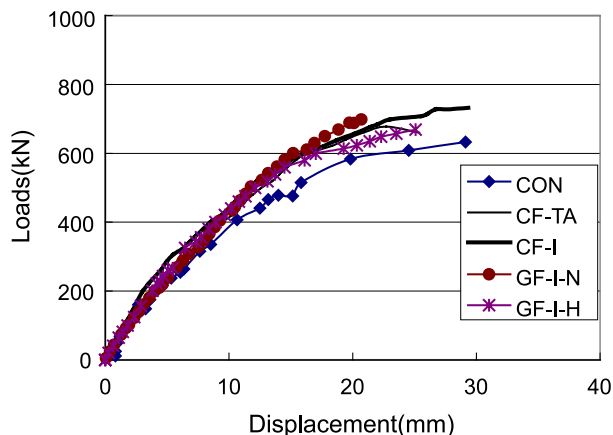


Fig. 9. Load–displacement relationship of decks strengthened with sheets.

ing material rather than on the rebar spacing or effective concrete cover, both of which have been traditionally accepted factors associated with the control of cracks. Failure of these panels was also due to punching shear, similar to panels CF-I and GF-I-N.

3.3. Load–displacement relationship

Figs. 8–10 show the load–displacement relationship mid-span for all 10 test panels. Panels SP-I and SP-I-H exhibited very similar behavior, with an almost linear deformation until failure. The stiffness of the deck strengthened with steel plate increased the most, among all of the strengthened deck panels, and displacement in the SP deck series were almost half that of the CON reference panel. Panel SP-I, for which the pre-loading was less than panel SP-I-H (270 kN, or 60% of the transverse rebar yield load), showed only a 10% decrease in load-carrying capacity, as compared to panel SP-I-H. Also, the stiffness of panel SP-I was greater than that of panel SP-I-H. Here, the slope of the load–displacement relationship prior to yielding or failure was defined as the structural stiffness.

Panel GP-I strengthened with GFRP had an elastic modulus that was 10 times smaller than that of steel plate, even though the strengthening ratio was 76% greater than

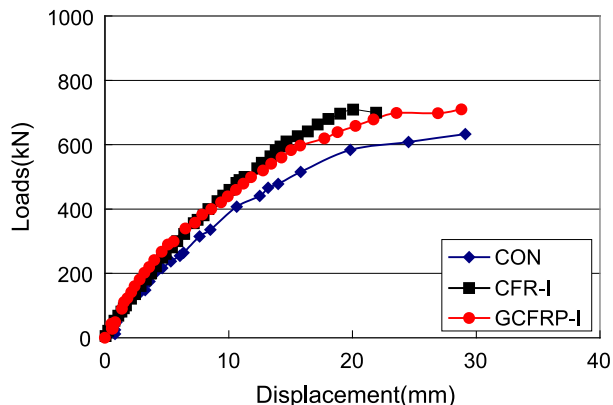


Fig. 10. Load–displacement relationship of decks strengthened with grids.

Table 3  
Comparison between theoretical results and test results

Specimen	Failure pattern	Theoretical load-carrying capacity (kN)			Test result (kN)		
		Beam theory (kNm/m)	Yield line theory		Punching shear	Yield	Failure
			Yield	Failure			
CON	Punching after rebar's yield	83	450		360	633	–
SP-I	Brittle punching shear	150	not yield	960	860	not yield	823
SP-I-H						not yield	758
GP-I	Brittle punching shear	150	not yield	990	780	not yield	813
CF-TA	Punching and interface debonding	185	not yield	470	380	not yield	684
CF-I	Punching after rebar's yield	132	620	740	400	690	732
GF-I-N	Punching and interface debonding	141	640	840	400	620	710
GF-I-H	Punching failure					600	669
CFR-I	Punching failure	190	not yield	1010	660	not yield	698
GCFRP-I	Punching after rebar's yield	169	720	910	430	700	710

Yield in the column of yield line theory means the yield load of longitudinal rebar after yield of transverse rebar.

Failure in the column of yield line theory means failure loads of strengthening material.

that of panels in the SP-I series, and the ultimate strengths of GFRP and steel plate were almost the same.

The stiffness of panels CF-TA and CF-I was slightly higher than that of panel CON, and their strengths were increased by 7% and 16% over that of panel CON, respectively. This indicates that two-directional strengthening with CFS strips is more effective than the scheme used for panel CF-TA, which used the same amount of CFS but in the transverse direction. This result is similar to that reported in a previous study by the authors. Also, increments in the punching shear strength of the strengthened panels are shown in the theoretical analysis, despite the inaccuracy of the theoretical strength (see Table 3), due to the fact that previous punching shear models neglected the restraint effect on the concrete of the strengthening material.

The load displacement relationships of panels GF-I-N and GF-I-H were very similar to panel CF-I. Panel GF-I-N did not receive any pre-loading, and was slightly less stiff than panel CF-I. The difference in strength between panels GF-I-N and GF-I-H was about 6%. This verifies that the strength decreases due to pre-damage can be ignored for static loads below the yield loads of rebar. If the quality of the repair work to structural damage such as a macro crack is reliable, the overall static response effect on the structure due to pre-damage will be minimal. A more important factor for the strengthening efficiency is not the existence of pre-damage, but the precision of the rehabilitation work.

Whereas the strengthening ratio of panel GCFRP-I were half those of panel CFR-I, ultimate strength of two specimens is almost same. Therefore, although panel CFR-I was calculated to have a higher load-carrying capacity than panel GCFRP-I, the actual punching shear strength of panel GCFRP-I was higher, and it was more ductile, since the reinforcing steel bars yielded in both directions prior to the punching shear failure.

#### 4. Discussion of test results

It is difficult to determine the load-carrying capacity of a strengthened deck because it depends on the type of loading, type of strengthening, and restraint conditions. Until now, traditional elastic beam theory, which considers a one-way slab of unit width, was used to design either the traditional deck or the strengthened bridge deck capacity; however, elastic beam theory is too simplistic to yield realistic results. Therefore, a simple, but reasonably accurate, analysis method is required as an alternative. Yield line theory and punching shear analysis described in Section 2 may be more suitable for this task [4]. From yield line theory, an analysis of panels CF-I, GF-I-N, and GCFRP-I, showed that the rebar in both directions yielded before the occurrence of punching shear failure. The theoretical yield loads agreed with the experimental results, except that the value for

Table 4  
Strain in the transverse rebar for every 100-kN load until failure ( $\times 10^{-6}$ )

	100 kN	200 kN	300 kN	400 kN	500 kN	600 kN	700 kN	800 kN
CON	436	944	1375	1966	6423	failure of gage		
SP-I	83	158	246	327	378	428	426	456
GP-I	110	311	596	939	1229	1479	1635	1859
CF-TA	286	590	924	1204	1569	1898		
CF-I	159	400	915	1348	1708	2446	failure of gage	
GF-I-N	298	664	1170	1630	1983	failure of gage		
CFR-I	68	323	620	1035	1434	1718	2004	
GCFRP-I	68	403	866	1358	1803	2754	7703	



Table 5  
Structural stiffness of strengthened panel

	Initial stiffness		Structural stiffness	
	$\frac{P_{20}}{\delta_{20}}$	$\frac{\text{Strengthened}}{\text{CON}}$	$\frac{P_{40}-P_{20}}{\delta_{40}-\delta_{20}}$	$\frac{\text{Strengthened}}{\text{CON}}$
CON	4.959	1.000	3.117	1.000
SP-I	7.693	1.551	8.996	2.886
SP-I-H	7.044	1.420	10.274	3.296
GP-I	6.783	1.368	4.942	1.585
CF-TA	5.100	1.028	3.675	1.179
CF-I	6.623	1.335	3.689	1.183
GF-I-N	5.768	1.163	3.366	1.080
GF-I-H	5.296	1.068	3.920	1.258
CFR-I	5.460	1.101	4.277	1.372
GCFRP-I	6.351	1.281	3.674	1.179

GCFRP-I was slightly higher than that observed for an actual load.

The punching shear strength given by Eq. (5) was only overestimated in panel SP-I and underestimated in other panels (CF series, GF series, CFR-I and GCFRP-I). This suggests that the punching shear strength of a strengthened panel with FRP is increased by the shear strength of the concrete cover between the rebar and strengthening materials, something that is usually neglected in traditional concrete slab analyses. The assumption that the shear strength of concrete cover is contributed to punching shear strength agrees with the test results.

Table 4 gives the change in the strain rate of the transverse reinforcing steel bar at the mid-span of each panel for every 100-kN load increment. In reference panel CON, and panels CF-I, GF-I-N, and CGFRP, which had a lower strengthening ratio, the transverse and longitudinal rebar yielded prior to the punching shear failure. Therefore, these panels had more of a ductile flexural failure mode, whereas other specimens collapsed due to brittle failure.

Table 5 summarize for all panels the initial stiffness ( $P_{20}/\delta_{20}$ ), defined as the 200-kN load as a cracking load, divided by the mid-span deflection produced by that load as well as the corresponding stiffness ( $P_{40}-P_{20}/\delta_{40}-\delta_{20}$ ) between 200 and 400 kN load levels. A 400-kN load is a yield load of transverse rebar of panel CON. In this paper, the stiffness is defined as  $P/\delta$ , where  $P$  is the load and  $\delta$  is the displacement at mid-span. The initial stiffness was higher for the panels strengthened with plate, such as SP and GFRP. The stiffness of panels SP-I and SP-I-H increased as the load increased, whereas the stiffness of the other panels decreased as the load increased. In the other materials, which were designed to resist only a unidirectional or orthogonal stress (GFRP was woven as  $0/+90^\circ$ ), the change in the stress orientation or distribution caused by increasing loads initiated kinking across the cracks in the direction of the FRP.

## 5. Conclusions

The results presented here lead to the following conclusions. All of the strengthening materials that were

attached to concrete bridge deck panels in this study substantially increased load-carrying capacity and flexural stiffness. In particular, the stiffness of panel SP-I, strengthened with steel plate, increased noticeably. The panels strengthened with FRP materials failed more often in a ductile mode, indicating that the failure developed after the rebar yielded.

The load-carrying capacities of panels SP-I and GP-I, which were strengthened with the highest strengthening ratios, were 30% greater than that of the unstrengthened reference panel CON. Also, the structural stiffness of panel SP-I was 300% greater than that of panel CON, and the ductility of panels CF-I and GCFRP-I was 20% greater than that of panel CON. From the test results, CF sheets and GCFRP were the more effective strengthening materials.

Yield line theory and punching shear analysis can be used to predict the load-carrying capacity of bridge decks, depending on the amount of strengthening employed. Yield line theory can be used to predict with reasonable accuracy the strength of bridge decks, even if these are strengthened with FRP. For the determination of the amount of strengthening needed to improve the load-carrying capacity of deteriorated deck panels, this theory is more effective than either traditional beam theory or FE analysis. However, a punching shear theory that reflects the restraint effects that are due to the strengthening material should be developed to determine the amount of strengthening that will provide the best results.

## Acknowledgments

This work was supported by the Post-Doctoral Fellowship Program of the Korea Science and Engineering Foundation (KOSEF).

## References

- [1] A. Kumar, A.A. Odeh, J.R. Myers, Repair, evaluation, maintenance, and rehabilitation research program, Technical Report, Cons. Eng. Res. Lab. (Army), Champaign, IL, USA 1990.
- [2] H. Takeshi, An outline of repairing and strengthening of RC deck slabs, *Bridge Found. Eng.* 26 (8) (1994) 105–108.
- [3] H.M. Westergaard, Computation of stresses in bridge slabs due to wheel loads, *Public Roads* 11 (1) (1930) 1–23.
- [4] K.W. Johansen, *Yield Line Theory*, Cemt Conc Asso, London, 2000.
- [5] R. Park, W.L. Gamble, *Reinforced Concrete Slabs*, 2nd ed., John Wiley & Sons, 2000.
- [6] M.P. Nielsen, *Limit Analysis and Concrete Plasticity*, 2nd ed., CRC Press, Boca Raton, FL, 1999.
- [7] R.N. Swamy, R. Jones, J.W. Bloxham, Structural behavior of reinforced concrete beams of strengthened by epoxy-bonded steel plates, *Struct. Eng.* 65A (2) (1987) 59–68.
- [8] R.N. Swamy, R. Jones, A. Charif, The effect of external plate reinforcement on the strengthening of structurally damaged RC beams, *Struct. Eng.* 67 (3) (1989) 45–56.

- [9] J.R. Yost, E.R. Schmeckpeper, Strength and serviceability of FRP grid reinforced bridge decks, *J. Bridge Eng.* 6 (6) (2001) 605–612.
- [10] H. Oh, J. Sim, C. Meyer, Experimental assessment of bridge deck panels strengthened with carbon fiber sheets, *Compos., Part B Eng.* 34 (6) (2003) 527–538.
- [11] Korea's Ministry of Construction and Transportation, Korean Highway Design Specification, 1996.
- [12] Y. Maeda, S. Matsui, Load-Carrying Capacity and Remaining Life of First-Built Composite Girder Bridge in Japan, *Proc. of Composite and Mixed Construction*, Japan, 1985, pp. 50–59.